Overview of Recent Experimental Studies on TRIAM-1M

K. N. Sato 1), H. Zushi 1), K. Nakamura 1), K. Hanada 1), M. Sakamoto 1), H. Idei 1), M. Hasegawa 1), S. Kawasaki 1), H. Nakashima 1), A. Higashijima 1), D. Thang 1), F. Wang 2), I. Rego 2), K. Sasaki 2), H. Xu 2), B. Rajendraprasad 2), M. Ogawa 2), K. Takagi 2), K. Nakashima 2), S. Nishi 2), T. Aoki 2), N. Kimura 2), Y. Inada 2), Y. Nozaki 2), Y. Wataya 2), H. Sakai 2), M. Matsubara 2), S. Watanabe 2), K. Goto 2), Y. Miyoshi 2), N. Yoshida 1), K. Tokunaga 1), T. Fujiwara 1), M. Miyamoto 2), M. Tokitani 2), K. Uehara 3), Y. Sadamoto 4), Y. Nakashima 5), Y. Higashizono 5), Y. Takase 6), A. Ejiri 6), S.Kado 6), T. Shikama 6), S.Iio 7) , T. Takeda 8), Y. Hirooka 9), T. Morisaki 9), Y. Nakamura 9), K. Toi 9), T. Fujimoto 10), A. Iwamae 10), T. Maekawa 10), M. Nagata 11), N. Nishino 12), O. Mitarai 13)

1) Advanced Fusion Research Center, Research Institute for Applied Mechanics, Kyushu University, Fukuoka, Japan,
2) Interdisciplinary Graduate School of Engineering Sciences, Kyushu University, Fukuoka, Japan,
3) Japan Atomic Energy Agency, Ibaragi, Japan
4) Joetsu University of Education, Niigata, Japan
5) University of Tsukuba, Ibaragi, Japan
6) The University of Tokyo, Tokyo, Japan
7) Tokyo Institute of Technology, Tokyo, Japan
8) The University of Electro-Communications, Tokyo, Japan
9) National Institute for Fusion Science (NIFS), Gifu, Japan
10) Kyoto University, Kyoto, Japan
11) University of Hyogo, Hyogo, Japan
12) Hiroshima University, Hiroshima, Japan
13) Kyushu Tokai University, Kumamoto, Japan

E-mail : satcho@triam.kyushu-u.ac.jp

Abstract An overview of recent experimental studies on TRIAM-1M is presented. Several issues of plasma-wall interaction including particle retention in wall materials, co-deposition, and impurity behavior are investigated. It has turned out that the particle behavior in one super long discharge is not equivalent with that of the summation of successive medium long term discharges. Also, a clear increase of the number of dust particles has been observed as a function of discharge time in the case of long term discharges. Some issues of current drive with lower hybrid frequency and of the combination with electron cyclotron frequency (ECCD) are studied. In addition, the ECCD experiment relevant to ITER has been carried out with high toroidal magnetic field (~6 T).

1. Introduction

Among the issues for the realization of nuclear fusion in the future, the characteristics of plasmas in steady state operation (SSO) is a quite important one to be investigated. The plasma properties in the high magnetic field (B_T) is also important to be studied from the viewpoint for obtaining high performance plasmas. In recent years, intensive studies with SSO and with high field operation have been carried out in TRIAM-1M, which is a small sized high toroidal field tokamak (R_0 =0.8 m, a×b=0.12 m × 0.18 m, B_T =8T), in order to obtain various knowledge with respect both to the issues of steady state and high field plasmas [1]. Particularly, studies on Plasma-Wall Interaction (PWI) with long/ultra-long term sustained plasmas and on the detailed characteristics by lower-hybrid current drive (LHCD) have been performed in this sense.

Studies on particle behavior by macroscopic and microscopic approach, the effect of co-deposition, comparison of dynamic and static retentions in long/ultra-long term discharges have been carried out, and the results are described in section 2-1. Behaviors of impurity and dust particles are intensively investigated. The results are presented in sections 2-2 and 2-3, respectively. In section 3, the results of extensive studies on the characteristics of LHCD in SSO are described. As a high field experiment, a remote steering antenna for the injection of electron cyclotron waves (for both ECH and ECCD) has been developed, and applied to the combination experiments of LH and EC waves. The bi-directional LHCD and counter ECCD experiments are carried out. These are presented in section 4-1 and 4-2.

Each details are also presented in the papers EX/P4-25 (PWI, impurity and dust behavior), EX/P6-5 (LHCD), and EX/P6-23 (bi-directional LHCD and counter ECCD) in this conference.

2. Detailed PWI Studies in the Ultra-Long Term Discharges

(see EX/P4-25 for details)

2.1 Particle Behavior, Co-Deposition, and Dynamic/Static Retention in Long/Ultra-Long Term Discharge

Understanding of the characteristics and mechanism in plasma-wall interaction (PWI) is one of the most critical issues to be studied especially from the viewpoint of steady state operation (SSO) of fusion plasmas both for ITER and future fusion reactors. In TRIAM-1M, which has a capability of SSO, the PWI experiments have been carried out extensively.

The ultra-long discharge with the duration of more than 5 hours was achieved in TRIAM-1M using a local movable limiter with good cooling capability (Fig.1). Detailed PWI studies have been extensively carried out using steady-state/ultra-long discharge plasmas with the discharge duration of the order of hours[1-3].

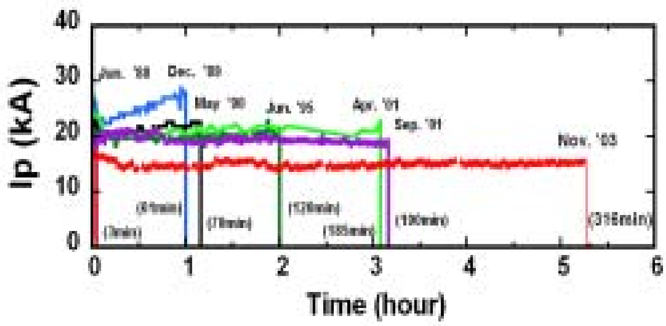

FIG. 1. Plasma current behavior of long term sustained discharges at various stages.

Effects of the movable limiter on the global wall recycling have been studied. Due to insertion of the movable limiter to the plasma edge, SOL parameters, the toroidal profile of the neutral particle density and the heat load on the wall have been changed to influence the global wall recycling. In the 5 hour discharge, the temperature increase in the plasma facing components has been successfully suppressed by the insertion of the movable limiter. Long time global wall saturation, i.e. global balance between particle absorption and release of the wall, has not been observed as compared with the case of 3 hour discharge, where the movable limiter was not applied and the temperature increases of the various wall materials during the discharge were much larger than the case with the movable limiter. The wall inventories and wall temperature increases as a function of time in the cases of 3 hour and 5 hour discharges are shown in Fig.2 [2].

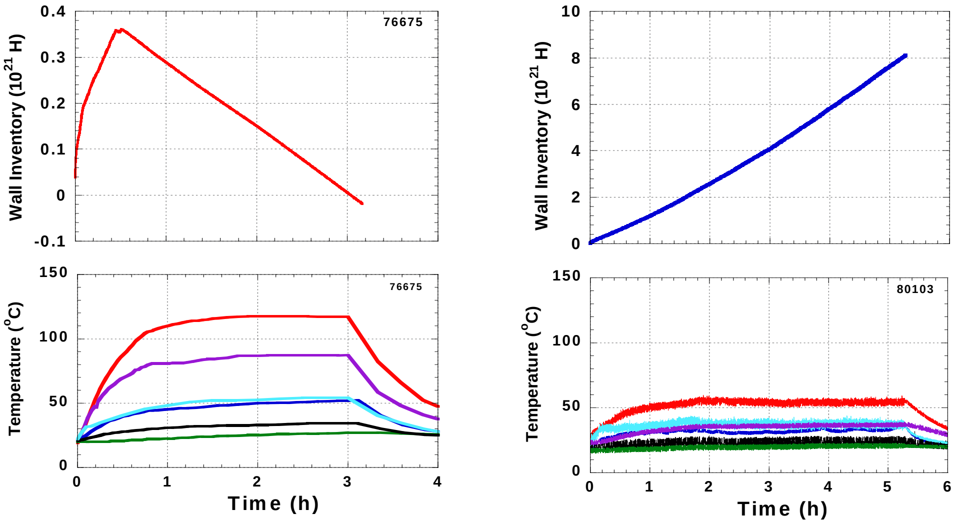

(a) (b)

FIG. 2. Wall inventories and wall temperature increases as a function of time are shown in the case of (a) 3 hour discharge and (b) 5 hour discharge.

Comparison of dynamic and static retentions, and effect of co-deposition have also been studied in detail [4]. The dynamic and static retentions; that is, the effective wall pumping rates analyzed by the global particle balance and by the results of surface probe measurement, have turned out to agree well with each other in spite of different measurement conditions.

Another valuable knowledge in PWI studies is the importance of co-deposition effect even in the device with all metal plasma facing components (PFC). Since new layer of limiter material (molybdenum in TRIAM-1M case) seems to be continuously created on the PFC, causing the infinite retention of hydrogen by co-deposition [5]. This will lead to the uncontrollability of particles in continuous operation, which has been confirmed in long term sustained discharges. The present result clearly means that the particle control in the future reactor would not be successful unless the recycling rate to be actively controlled and kept to be nearly unity. In this sense, a concept of actively temperature-controlled PFC will be one of the important approaches in the fusion reactor.

In addition, various phenomena of PWI in long duration discharges have been investigated focusing on their length scales. The scales are classified according to the length from the order of a diameter of the torus to that of the microstructure of the deposits on the wall. One of the key phenomena to bridge between the scales is co-deposition of hydrogen with the eroded atoms [6].

2.2 Impurity Behavior in the Ultra-Long Term Discharge [7]

Another important result obtained through the analysis of long term discharges is that the particle behavior in one ultra-long discharge is not equivalent with that of the summation of successive medium long term discharges.

The oxygen behavior during the ultra-long term discharge and between the two long term discharges have been extensively studied in order to know PWI characteristics in this sense. Figure 3 shows the comparison of time behavior of the OII intensity (I_{OII}) normalized by the electron density (n_e) in the case of one ultra-long term discharge (Fig.3(a)) and that of the summation of successive medium long term discharges ignoring time intervals of every

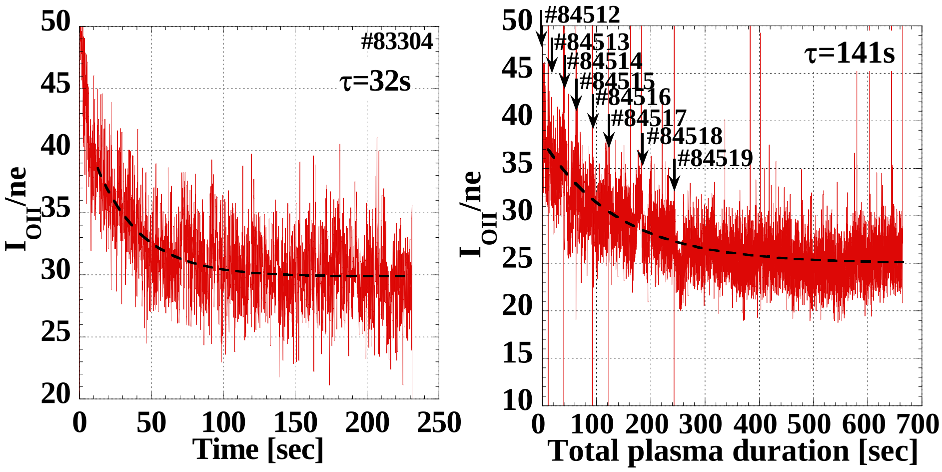

(a) (b)

FIG.3. Comparison of time behavior of OII intensity (I_{OII}) normalized by the electron density (n_e) in the case of one super long term discharge (a) and that of the summation of successive medium long term discharges (b).

discharges concerned (Fig3(b)), where I_{OII} /n_e represents a measure of an oxygen influx from the surface of PFC with a certain assumption. Here, the time constant in the case of Fig.3(a) is 32 sec, whereas that in the case of Fig.3(b) is 141 sec, which is quite larger by a factor of 4-5.

Further analysis shows that time interval between two discharges has a strong effect to the increase of I_{OII} /n_e. The modeling study shows that the phenomena will be explained by the

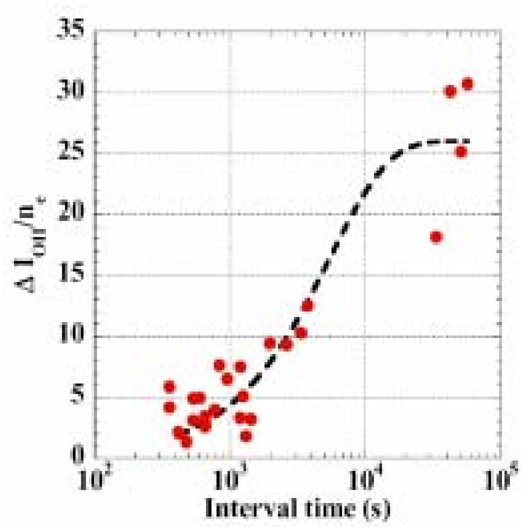

FIG..4. Influence of the interval time on the value of I_{OII}/ne at the beginning of the discharge. The broken line is a fitting curve according to the equation above. Here, ΔI_{OII}/ne has increased with the time constant of 5500 s.

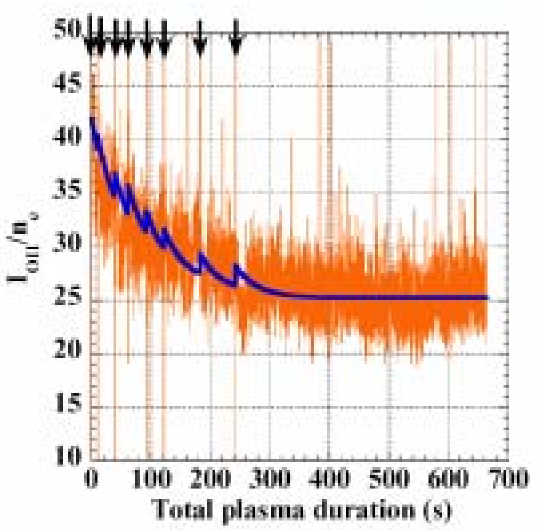

FIG.5. The result of modeling of the repetition of discharges. The solid line is the result of modeling. The arrows mean the beginning of each discharge. It has turned out that the modeling well reproduces the experimental result.

transport of oxygens followed by Langmuir's isotherm during the time interval, and the increase Δ of I_{OII} /n_e during the time interval has a relation as

$$\Delta I_{OII}/n_e \propto 1 - \exp(-t/\tau)$$

with τ = 5500 sec (Fig.4). Also, a modeling of the repetition of discharges has been performed, and it has turned out that the modeling has well reproduced the experimental results. The time constant of decrease in the case of Fig.3(b) in the modeling has become to be 112 s (Fig.5), which is quite consistent with the experimental result.

Thus, it has turned out that the PWI characteristics in ultra-long term discharge cannot be reproduced by the repetition of short or medium term discharges, and the dependence of particle behavior on the duty cycle should be one of the quite important factors both in ITER and in a future reactor.

2.3 Behavior of Dust Particles in the Long Term Discharge [8]

Recent years, quite large attention has been paid to the behavior of dust particles in vacuum vessels in the fusion plasma experiments. The effects of dust behavior are significant on the performance of core and boundary plasmas as well as on the issue of hydrogen/tritium retention from the viewpoints of global particle control in steady state operation and of the tritium inventory in future devices. The studies on dust particles have been carried out in various places, however, the mechanism of generation and detailed behavior are not clarified yet.

As non-regular events the dust particle studies have been carried out by using a high speed framing camera system as shown in Fig.6. A typical result is shown in Fig.7, which clearly shows a rapid increase of dust particles as a function of discharge duration in steady state operation. Velocities of dust particles observed by the high speed camera are in the range of 10~50 m/sec. On the other hand, those directions seem to scatter without a certain tendency. Also, various characteristics of dust particles; i.e. distributions of size, shape, the number on unit area, location, and species, are systematically being studied by collecting from the vacuum vessel after the last experimental campaign. The distribution of size is shown in Fig.8. It seems there are typically two types in shape, flake-type and sphere-type ones. The composition has turned out to be mainly molybdenum and SUS through the analysis with the scanning electron microscope (SEM).

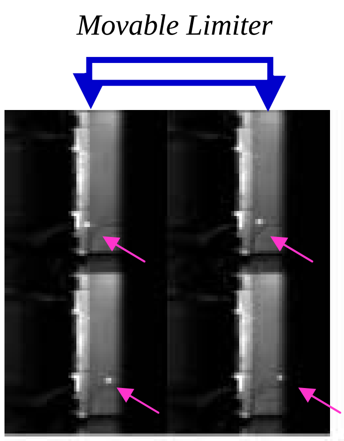

FIG.6. An example of a dust particle behavior observed by the high speed framing camera system.

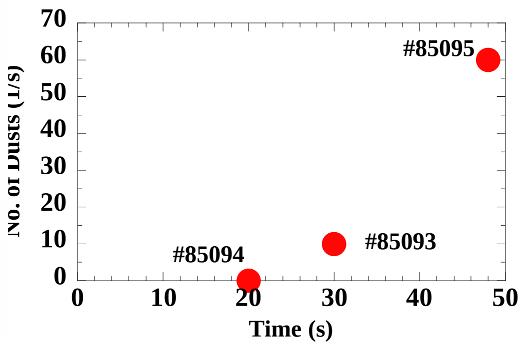

FIG.7. The number of dust particles as a function of discharge duration observed by the high speed framing camera system..

Sometimes, a hot spot is observed on the movable limiter as shown in Fig.9, where dust particles are confirmed to come out intensively from the surface. Spectroscopic measurements have been simultaneously carried out to have the information of highly ionized Mo (Mo XIII)

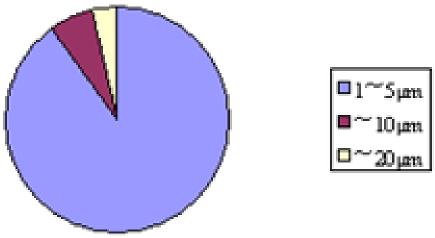

FIG.8. Distribution of dust particle size which has been collected after the last experimental campaign

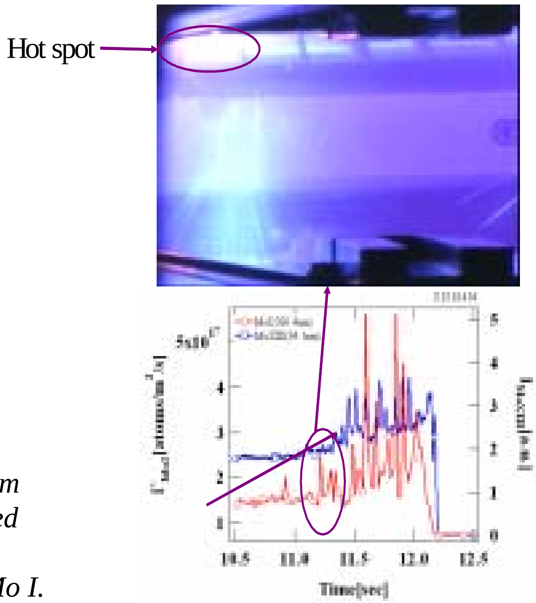

FIG.9. A hot spot observed on the movable limiter, from the surface of which dust particles are observed to come out intensively (top). Also, results of spectroscopic measurements of Mo XIII and Mo I. [right]

and Mo atoms (Mo I), and the molybdenum neutral flux has been analyzed from the data of Mo I (Fig.9). The increase and rapidly oscillating behavior both in Mo XIII intensity and flux of Γ (Mo I) have occasionally been observed just before the discharge termination. Long duration discharges have terminated without a clear cause. However, it sometimes happens at a certain phase of very low frequency PWI events, which corresponds to the phase of maximum intensities of Hα and Mo XIII. This might suggest the introduction of dust particles to be a possible cause of discharge termination.

3. Lower Hybrid Current Drive Characteristics in Long Term/Steady State Discharge

(see EX/P6-5 for details)

As is commonly understood, the current drive in tokamak is inevitable to be developed. The lower hybrid current drive (LHCD) is an important and powerful tool for non-inductively sustaining plasma current, and the full LHCD plasmas have been studied in many tokamak devices. Recently LHCD in the high density region, that is in ITER relevant region (~ 1×10^{20} m^{-3}), was reported on FTU [9]. A steady-state full LHCD discharge in intermediate density was achieved on Tore Supra and total injected energy reached up to beyond 1 GJ [10]. A 5 hour discharge was obtained in low density region on TRIAM-1M [1-3].

On TRIAM-1M, full LHCD plasmas have been obtained in the wide ranges of line-averaged electron density, $n_e = 0.1\text{-}4.7 \times 10^{19}\ m^{-3}$, plasma current, $I_P = 15\text{-}100$ kA, and injected power, $P_{LH} = 0.003\text{-}0.2$ MW. The power dependence of achieved density and current drive efficiency are reported and a simple model is introduced to explain the tendency [11].

The region of pure LHCD plasmas are summarized in I_p (plasma current) – P_{rf} (radio frequency power) space as shown in Fig.10, where the region of I_p more than 80 kA is the recently obtained one. The highest current of about 100 kA, which

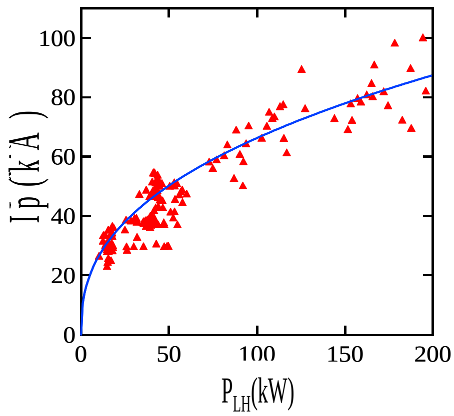

FIG.10. Recent experimental region of plasma current Ip vs LH-power P_{LH} in TRIAM-1M.

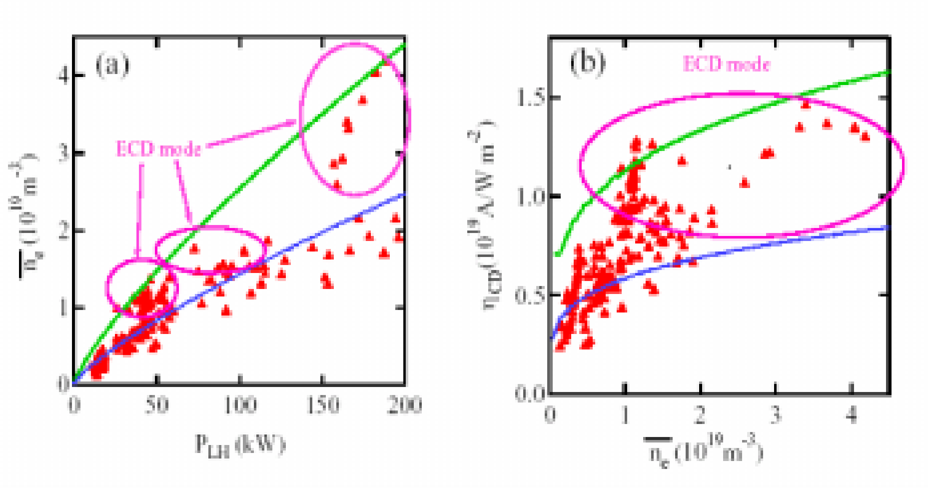

FIG.11. (a) The densities at the time of the peak plasma current during full LHCD are plotted as a function of injected power. The solid (L-mode) and dotted (L-mode x 0.8) lines show the calculated value based on the model in Ref.[11]. Ellipses show the regions of the ECD (Enhanced Current Drive mode [12]) plasma. (b): The current drive efficiencies as a function of electron density. The ellipses show the region of ECD plasma.

corresponds to be a state of q < 4, has been obtained. Although the fitting curve has a relation of $I_p \propto P_{rf}^{0.4}$, the mechanism underlying is not known.

The power dependence of density has also been investigated in full LHCD plasma; here the achieved average n_e depends on P_{LH}, as shown in Fig.11(a). The solid (L-mode) and dotted (L-mode x 0.8) lines show the calculated value based on the model in Ref.[11]. The dependence is similar to the data except enhanced current drive (ECD) mode [12], where τ_e and η_{CD} are better than no ECD case. On TRIAM-1M, the current drive efficiency η_{CD} increases with the density as shown in Fig. 11(b). This is not predicted by the Fisch's LHCD theory [13]. The solid and dotted lines show the similar ones as in Fig.11(a).

Strong gas-puff makes a termination of the discharge in high density region, where the density is still much lower than the limit predicted by wave propagation characteristics. The achieved average n_e and the current drive efficiency η_{CD} have a significant relation to P_{LH}, and their power dependences are close to the one predicted by a model derived from the balance between the energy confinement τ_E and η_{CD} of the LHCD scaling. This density limit depends on the injected P_{LH}. The limit will appear in full CD discharges, including ECCD, NBCD, and bootstrap current, and it wanes with the increase of the portion of the ohmic heating power.

The power dependences of density and plasma current in full LHCD discharges are obtained. Especially the density in full LHCD plasma is not limited by the wave propagation condition, but by the balance between the plasma confinement and the current drive efficiency. The model can obtain the dependence of current drive efficiency on density, which is not predicted by the current drive theory. The model does not have contradiction with the observation of the transition to the ECD mode on TRIAM-1M [12].

4. High B_T Experiments with ECCD and LHCD

4.1 Development of Remote Steering Antenna for High B_T - ECCD Relevant to ITER

Electron Cyclotron Heating and Current Drive (ECH/ECCD) is an auxiliary heating and CD systems for the International Thermonuclear Experimental Reactor (ITER). A total power of 20MW at a frequency of 170 GHz will be injected from the upper and the mid-plane ports at the low field side of the ITER. A remote steering antenna concept has been proposed for the ITER application [14,15], so that the plasma-facing movable mirrors do not have to be installed. The remote steering antenna was considered as the upper port launcher in the ITER [16].

The TRIAM-1M tokamak has super-conducting magnetic coils, which generate a high field up to 8T. Using the features of the super-conducting tokamak, the steady-state plasma operation with the Lower Hybrid Current Drive (LHCD) has been demonstrated [1,2]. The ECH system with a 170 GHz gyrotron was prepared for the ECH experiments with a fundamental heating scenario [17]. The plasma current was initiated solely by radio frequency [Electron Cyclotron (EC) and Lower Hybrid (LH)] waves in the tokamak [17,18]. For the ECCD experiment, a new antenna system is necessary to control the launching angle. In the TRIAM-1M tokamak, the device port has insufficient space to install a mirror array to the vessel due to the large bell jar of the magnet coils. A remote-steering antenna system has recently been developed for the tokamak experiments.

In general, there are two operation modes in a remote steering antenna; the anti-symmetric and symmetric modes. The anti-symmetric and symmetric directions are defined for the anti-symmetric or symmetric property of the output beam-axis for the incident steering beam-axis. Figure 12 shows the matching coefficient $C_{\mathrm{in,out}}$ of the imaging property calculation in an anti-symmetric direction antenna, and in a symmetric antenna with an extended steering-angle capability, when the electric field is perpendicular to the steering plane. The matching coefficient $C_{\mathrm{in,out}}$ is defined as follows:

$$C_{\mathrm{in,out}} = \frac{\left|\int E_{\mathrm{in}}(x,y)E^{*}_{\mathrm{out}}(x,y)\mathrm{d}x\mathrm{d}y\right|^2}{\int |E_{\mathrm{in}}(x,y)|^2\mathrm{d}x\mathrm{d}y \cdot \int |E_{\mathrm{out}}(x,y)|^2\mathrm{d}x\mathrm{d}y},$$

where $E_{\mathrm{in}}(x,y)$ and $E_{\mathrm{out}}(x,y)$ are input Gaussian beam field and output hybrid mode field, respectively. In the anti-symmetric case, the matching coefficient $C_{\mathrm{in,out}}$ should be evaluated using $E_{\mathrm{in}}(x,y)$ with the minus angle for the input steering angle. The lengths of the anti-symmetric and symmetric antennas are 2.245 m and 2.075 m, respectively. A side of the square is fixed at 31.75 mm. The anti-symmetric direction antenna of the ITER-type antenna operates up to 12 degrees. The symmetric direction antenna, which has an extended steering-angle capability, operates at angles near 0 degrees and with larger steering angles between 8-19 degrees. This new operation region has recently been found [19]. The symmetric direction antenna with L=2.075m, which have perpendicular and oblique injection capability, is useful for both the ECH and ECCD experiments in the TRIAM-1M tokamak.

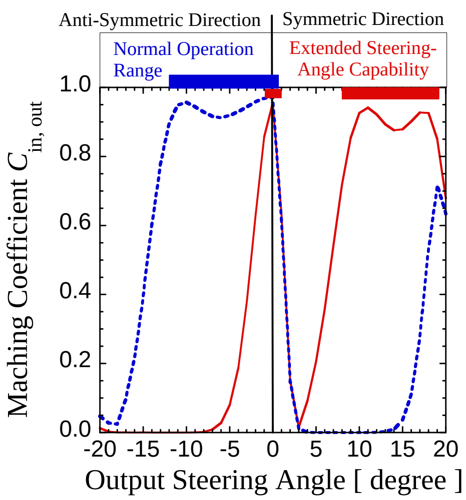

FIG.12. Matching coefficient $C_{in,out}$ of the imaging property calculation in an anti-symmetric direction antenna, and in a symmetric antenna with an extended steering-angle capability.

The antenna performance has been tested at the low power test facilities. Figure 13 shows the intensity and phase profiles in the x direction for the perpendicular component to the steering x-z plane at the z = 65 mm in the 15 degree steering case. The coordinate (x, y, z) is shown in the figure. The intensity profile was a Gaussian-like beam of w_x = 11 mm. However, there was a side lobe. The phase profile was parabolic with a phase curvature of R_x = 218 mm in the main lobe, but, was not explained with the parabolic Gaussian. The radiated field E_{rad} (x_1, y_1) was evaluated by the Huygens-Kirchhoff integral calculation using the output hybrid mode filed at the antenna exit E_{out} (x_2,y_2) as follows:

$$
\begin{aligned}
E_{\rm rad}(x_2, y_2, z_1) &= \frac{i}{\lambda}\int\!\!\int E_{\rm out}(x_1, y_1)\frac{\exp\left(-i\frac{2\pi r}{\lambda}\right)}{r}dx_1dy_1, \\
r &= \sqrt{(x_2-x_1)^2+(y_2-y_1)^2+z_1^2},
\end{aligned}
$$

where r is the distance between the antenna exit position (x_1, y_1, 0) and radiated position (x_2, y_2, , z_1). The calculated field is also shown in the figure. The beam centers measured and calculated fields are offset, and the beam size in the calculated field is similar to the measured size. The measured phase profile is explained very well with the calculated phase profile. The radiation field from the developed antenna in the extended steering angle can be explained with the calculated field by the Huygens-Kirchhoff integral.

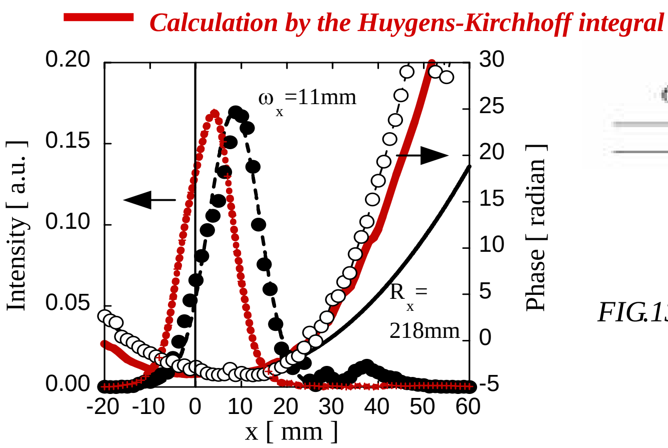

FIG.13. Measured and calculated intensity and phase profiles in the 15 degree steering case.

By using the remote steering antenna system, fundamental ECH and ECCD experiments have been conducted in the ITER frequency from the low field side. In addition, the experimental studies on O-mode and X-mode ECCD have been carried out especially as a high field experiment relevant to ITER [20]. These results show that efficiency increase of LHCD through bulk electron heating seems to be dominant in O-mode case, whereas the ECCD effect by coupling to the fast electrons is clearly seen in X-mode case.

In the X-mode experiment, clear differences in the plasma current and the hard X-ray intensity have been observed between the co- and counter- steering injections due to the ECCD effect on the coupling of fast electrons in the LHCD plasmas. The X-mode ECCD has been used to the bi-directional CD study, whish is described in the next session.

4.2 Bi-Directional LHCD and the Counter ECCD in Full LHCD Plasmas

(see EX/P6-23 for details)

The bi-directional LHCD and the electron cyclotron counter current drive (counter ECCD) experiments have been carried out in order to study the controllability for current profiles and to investigate the spectrum gap problem. The interesting results have been obtained, which includes different effects with respect to backward LH and ECCD [21].

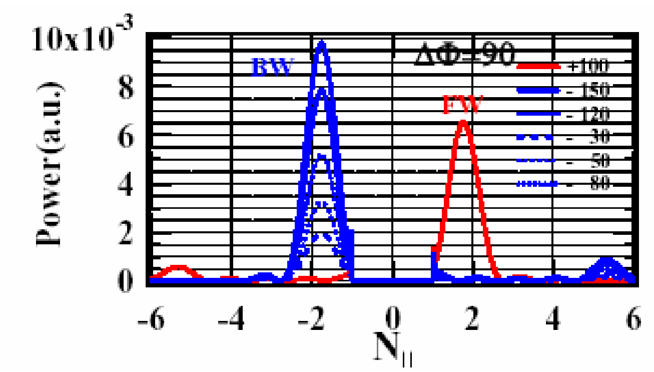

FIG.14. Power spectra for FW- (right) and BW- (left) LH waves The antenna phasing is ±π/2.

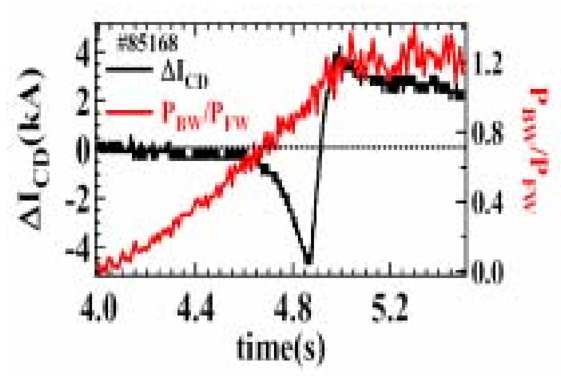

FIG.15. Change in driven current and power ratio $\alpha = P_{BWLH}/P_{FWLH}$ are plotted as a function of time.

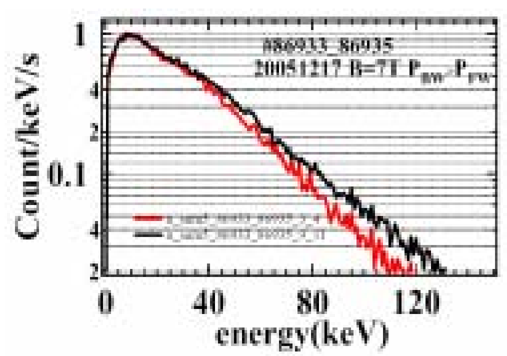

FIG.16. Hard X-ray energy spectra for FW-LH (below) and FW-LH+BW-LH (above) cases. The sampling time is 1 sec.

Combined experiments with lower hybrid (LH) and electron cyclotron (EC) waves have been carried out in order to study the counter current drive in full LHCD plasmas.

Two sets of the 8.2 GHz RF system each having 8 klystrons of 25 kW each have been utilized. Both backward (BW) and forward (FW) LH waves are launched from identical grill antennas, which are toroidally apart from each other by 180 degree. The phasing of grill antenna is ±90 degree, whose peak refractive index N_{II}^{peak} is ~ ±1.65 corresponding to resonant electron energy of ~100 keV. The spectra with the width $\Delta N_{II}/N_{II}$ ~ 1 is shown in Fig.14. In the experiments the target plasma is sustained for ~ 10 sec by FW-LH wave in steady state with the fixed power P_{FWLH} of ~ 40 keV. On the other hand, the BW-LH wave has been injected at the stationary phase, and the power P_{BWLH} has been varied in time with the maximum rate of the power ramp being ~ 80 kW/sec and the maximum power ratio being ~ 1.5 during the bi-directional CD phase, as shown in Fig.15.

With injection of the BW-LH wave the counter current drive depends on the power ratio of BW-LH wave and FW-LH wave ($\alpha = P_{BWLH}/P_{FWLH}$). For $\alpha < 1$, counter CD is confirmed by the reduction of driven current. A transition in current drive scheme seems to occur near $\alpha \sim 1$, and the net increase in co-current is observed for $\alpha > 1$. Relativistic resonant interaction between BW-ECW and counter-passing electrons has been confirmed by the acceleration in hard X-ray energy spectrum (Fig.16). This interaction, therefore, has caused the current in co-direction to enhance by a factor of ~ 50 %.

The dependence of the resonance location has been studied. For inboard off-axis condition counter current drive with large Shafranov shift is achieved, but for on-axis and outboard off-axis cases increment in co-current is obtained. For on-axis condition, however, net counter-current is achieved as α increases. The Ohkawa scheme seems to be plausible for outboard off-axis case.

5. Concluding Remarks

The characteristics of plasmas in steady state operation (SSO) is a quite important issue to be investigated for the future fusion reactor. The plasma properties in high magnetic field is also important to be studied from the viewpoint for obtaining high performance plasmas.

In recent years, intensive studies with SSO and with high field operation have been carried out in TRIAM-1M in order to obtain various knowledge with respect both to the issues of steady state and high field plasmas. Particularly, studies on Plasma-Wall Interaction (PWI) in the ultra-long term sustained plasmas and on the detailed characteristics with lower-hybrid current drive (LHCD) have been performed in this sense.

The detailed studies on PWI have been carried out using steady-state/ultra-long discharge plasmas with the discharge duration of the order of hours. Studies on particle behavior by macroscopic and microscopic approach, the effect of co-deposition, comparison of dynamic and static retentions in long/ultra-long term discharges have been carried out, and the useful results are obtained.

Comparison of dynamic and static retentions, and effect of co-deposition have also been studied in detail. The dynamic and static retentions have turned out to agree well with each other in spite of different measurement conditions.

The importance of co-deposition effect has turned out to be significant even in the device with all metal PFC as in TRIAM-1M. Since new layer of limiter material will be continuously created on the PFC, the retention of hydrogen may become infinite by co-deposition. This will lead to the uncontrollability of particles in SSO. This clearly means that the particle control in the future reactor would not be successful unless the recycling rate to be actively controlled and kept to be nearly unity.

Another important result obtained through the analysis of long term discharges is that the particle behavior in one ultra-long discharge is not equivalent with that of the summation of successive medium long term discharges. Thus, it has turned out that the PWI characteristics in ultra-long term discharge cannot be reproduced by the repetition of short or medium term discharges, and the dependence of particle behavior on the duty cycle should be one of the important factors both in ITER and in a future reactor.

Behaviors of impurity and dust particles are intensively investigated. The dust particles have been observed by using a high speed framing camera system. A typical result shows a rapid increase of dust particles as a function of discharge duration in steady state operation. Velocities and directions of flying dust particles are measured. Also, various characteristics of dust particles; i.e. distributions of size, shape, the number on unit area, location, and species, are systematically studied by collecting from the vacuum vessel after the last experimental campaign.

Long duration discharges have terminated without a clear cause. Although it sometimes happens that the termination occurs at the timing of strong intensities of Hα and MoXIII, the conclusion should be derived with careful consideration.

Full lower hybrid current drive (LHCD) plasmas on TRIAM-1M have been investigated in the wide ranges of line-averaged electron density, n_e = 0.1-4.7x10^{19} m^{-3}, plasma current, I_P = 15-100 kA, and injected power, P_{LH} = 0.003-0.2 MW. Strong gas-puff makes a termination of the discharge in high density region, where the density is still much lower than the limit predicted by wave propagation characteristics. However, a model derived from the balance between the energy confinement, τ_E, and η_{CD} of the LHCD scaling might predict the difference.

For the ECCD experiment, the antenna system with the controllability of launching angle is necessary, and a remote-steering antenna system has been developed. By using this system the bi-directional LHCD and the counter ECCD experiments have been carried out in order to study the controllability for current profiles and to investigate the spectrum gap problem in the sense of both obtaining physics understanding as well as improving CD efficiency or exploring new regime of CD. Quite interesting results have been obtained, which includes different effects with respect to backward LH and ECCD.

Acknowledgement

This work is partially carried out under the framework both of the Joint-Use Research at RIAM, Kyushu University and of the Bilateral Collaboration Research organized by National Institute for Fusion Science, Japan. This work is partially supported by the Grant-in-Aid for Scientific Research from the Ministry of Education, Culture, Sports, Science and Technology of Japan.

References

[1] H. Zushi et al., Nucl. Fusion **45** (2005) S142.
[2] M. Sakamoto et al., 32nd EPS Conf. (Tarragona, 2005) P5-005.
[3] K. Hanada, et al., Fusion Engineering and design **81** (2006) 2257.
[4] M. Sakamoto et al., J. Nuclear Materials **313-316** (2003) 519.
[5] M. Sakamoto et al., Nucl. Fusion **44** (2004) 693.
[6] M. Sakamoto et al., this conference: EX/P4-25.
[7] M. Ogawa et al., Int. Conf. of PSI (Chengdu, 2006) P2-73.
[8] K. Sasaki et al., Int. Conf. of PSI (Chengdu, 2006) P1-27.
[9] G. Granucci et al., Fusion Science &Tech. **45** (2004) 387.
V.Pericoli-Ridolfini et al., Phys. Rev. Lett. **82** (1999) 93.
[10] J. Jacquinot, Nucl. Fusion **45** (2005) S118-S131.
[11] K. Hanada et al., this conference: EX/P6-5.
[12] K. Hanada et al., Nulc. Fusion, **41**(2001) 1539.
[13] N. Fisch, Phys. Rev. Lett. **41** (1978) 873, N. Fisch, Rev. of Modern Phys. **59** (1987) 175.
[14] R. Prater et al., 1997 Proc. of 10th Joint WS on Electron Cyclotron Emission and Electron Cyclotron Resonance Heating, World Scientific Pub Co Inc., p531.
[15] C. P. Moeller, 1998 Proc. of the 23rd Int. Conf. on IR and MWW, p116.
[16] A. Verhoeven et al., J. Phys.: Conf. Ser. **25** (2005) 84.
[17] M. Hasegawa et al., J. Plasma Fusion Res. **80** (2003) 53.
[18] K. Hanada et al., Nuclear Fusion, **44** (2004) 357.
[19] K. Ohkubo et al., Fusion Eng, and Des. **65** (2003) 657.
[20] H. Idei et al., Nuclear Fusion **46** (2006) 489.
[21] H. Zushi et al., this conference: EX/P6-23.